Original Research

Butyrate reduces high-fat diet-induced metabolic alterations, hepatic steatosis and pancreatic beta cell and intestinal barrier dysfunctions in prediabetic mice

VA Matheus, LCS Monteiro, RB Oliveira, DA Maschio and CB Collares-Buzato

Department of Biochemistry and Tissue Biology, Institute of Biology, University of Campinas (UNICAMP), Campinas, São Paulo, CEP 13083-970, Brazil

Corresponding author: CB Collares-Buzato. Email: collares@unicamp.br

Impact statement

Butyrate is a short-chain fatty acid produced by the intestinal microbiota through the fermentation of non-absorbable carbohydrates and proteins (e.g. fibers). Sodium butyrate incorporated into the diet displayed a protective action on metabolic, hepatic, pancreatic and intestinal alterations induced by high-fat diet in mice, resulting in significant inhibition of the development of a prediabetic state. Thus, our data suggest that butyrate may have a potential therapeutic use in the treatment of type 2 diabetes and related disorders.

Abstract

In this study, we investigated the effect of diet supplementation with sodium butyrate (5% w/w), a short-chain fatty acid produced by the intestinal microbiota, on metabolic parameters, body adiposity, hepatic and pancreatic lipid accumulation, beta cell function/mass as well as on the structure and function of the tight junction-mediated intestinal epithelial barrier in both normal and obese/prediabetic C57 mice fed a regular (control) or high-fat diet for 60 days, respectively. Butyrate treatment significantly inhibited all the high-fat-induced metabolic dysfunctions evaluated, i.e. significantly reduced the weight gain and body adiposity as well as the insulin resistant state, hyperglycemia and hyperinsulinemia, without changing food intake. In addition, high-fat-fed mice treated with this short-chain fatty acid displayed no compensatory hyperplasia of pancreatic beta cells nor marked hepatic steatosis as seen in prediabetic mice after high-fat diet only. Isolated pancreatic islets from high-fat-fed mice treated with butyrate showed improvement of the insulin secretion, which was associated with a significant decrease in lipid accumulation within the pancreas. Butyrate enhanced the intestinal epithelial barrier, as revealed by the FITC-Dextran permeability assay, which was accompanied by a significant increase in the junctional content of the tight junction-associated claudin-1 in intestinal epithelia of jejunum, ileum, and colon of both control and high-fat mice. In conclusion, our results showed that diet supplementation with butyrate inhibits the deleterious effects of high-fat diet intake on metabolic parameters and structure/function of several tissues/organs associated with type 2 diabetes mellitus in a mouse model, suggesting a potential use of this short-chain fatty acid in the treatment of this endocrine-metabolic disorder.

Keywords: Butyrate, intestinal paracellular barrier, obesity, pancreatic beta cell, type 2 diabetes mellitus, high-fat diet

Experimental Biology and Medicine **2017; 242: 1214–1226. DOI: 10.1177/1535370217708188**

Introduction

Diabetes mellitus is a disorder that affects the metabolism of carbohydrates (in particular, glucose) as well as of lipids and proteins, as result of either a deficiency in insulin secretion or reduced sensitivity of tissues to this hormone.[1] There are two forms of diabetes, type 1 (T1DM) and type 2 diabetes mellitus (T2DM), that have distinct pathogenesis. T1DM is an autoimmune disease that results from a combination of genetic susceptibility, immune dysregulation and exposure to certain environmental factors (such as viral infection, dietary substances, etc.), leading to beta cell death and, as a consequence, in a deficiency of insulin production.[2,3] T2DM has a more complex etiology/pathogenesis and a higher incidence/prevalence in the world population nowadays. It is established that physical inactivity and obesity are important contributors to the onset of this disease, although there may be genetic and environmental predisposing factors associated with T2DM.[4,5]

Insulin resistance is one of the first signs of T2DM, being characterized by a general decrease in cell sensitivity to insulin, that leads to hyperglycemia due to reduced glucose uptake (mainly in muscle and adipose tissue) or increased glucose output (such as in the liver).[6–8] Although it is not

completely known which factors trigger the insulin resistance, high levels of circulating fatty acids and adipose tissue-derived pro-inflammatory cytokines certainly contribute to this condition.[4,6,9,10] In addition, it has been recently proposed that microbiota-derived lipopolysaccharides, crossing a leaky intestinal epithelium, may also play a role in the long-term development of insulin resistance in T2DM.[11–14]

In order to compensate the permanent state of insulin resistance, pancreatic beta cells are capable of an adaptive response that involves changes in their secretory function and mass in the endocrine pancreas.[15–18] At initial stages, beta cells increase insulin biosynthesis and release but, subsequently, due to the continuous resistance of biological tissues to insulin, beta cell mass expands to promote a further increase in secretion of this hormone necessary for the maintenance of normoglycemia.[15,17–19] In advanced stages, the constant demand for insulin hypersecretion in association with long-term exposition to hyperglycemia/dyslipidemia and a chronic inflammatory state within the pancreatic islet milieu result in secretory impairment and then beta-cell death by apoptosis, reducing its mass in the pancreas.[5,15–17,20,21] As a consequence, replacement therapy with insulin is needed to recover glucose homeostasis.

In addition to hormone replacement treatment of T2DM, alternative therapies have been proposed, particularly at the early stages of this disease, in order to control obesity and altered metabolism of carbohydrates, leading to a reversal of the prediabetic state. These therapies involve regular physical exercise and special diets and the intake of prebiotic and probiotic in view of the recent discovery of a possible association between microbiota and the development of diabetes.[12,22–28]

Butyrate is a short-chain fatty acid (SCFA) produced by the intestinal microbiota through the fermentation of non-absorbable carbohydrates and proteins (e.g. fibers). It has been demonstrated that butyrate has beneficial effects on intestinal mucosa, displaying anti-inflammatory, anti-oxidant and anti-carcinogenic actions.[29–33] In vitro conditions, butyrate induces an increase in the tight junction (TJ)-mediated epithelial barrier function by increasing the expression of the TJ-associated claudin-1 in intestinal cell line.[34] Regarding its systemic effect, there has been recently suggested an anti-diabetogenic effect of this SCFA in animal models of T1DM and T2DM, which was related to its action as histone deacetylase (HDAC) inhibitor.[31,35–39] Nevertheless, to the best of our knowledge, there is no study looking at the relationship between the effect of butyrate on the T2DM-associated metabolic, hepatic and pancreatic alterations and its action on the TJ-mediated intestinal epithelial barrier. Therefore, the aim of the present work was to investigate the effect of diet supplementation with sodium butyrate on metabolic parameters, adiposity, hepatic and pancreatic lipid accumulation, beta cell function/mass as well as on the structure and function of the intestinal epithelial barrier of obese and prediabetic mice.

Materials and methods

Animals and diets

Male C57BL/6JUnib mice (aged four to five months) were obtained from the breeding colonies of the Multidisciplinary Center for Biological Investigation on Laboratory Animal Science (CEMIB) of the University of Campinas (UNICAMP, Brazil). The animals were divided into four experimental groups: control (C), control + butyrate (CB), high-fat (HF) diet and HF diet + butyrate (HFB). Sodium butyrate (cat number 303410, Sigma) was incorporated into the regular and HF diets at a concentration of 5% (w/w) as previously described.[39] The C group received a standard rodent diet (in powder) (containing 4.5% lipids, 53% carbohydrates, and 23% proteins; w/w). The CB group received the standard diet mixed with 5% of sodium butyrate (w/w). Animals from the HF group received a prepared HF diet (in powder) (containing 21% lipids, 50% carbohydrates, and 20% proteins; w/w), while the HFB group received the same HF diet but mixed with 5% of sodium butyrate (w/w). The lipid composition of the HF diet was mainly lard (20 g/100 g diet), but also contained soy oil (1 mL/100 g diet). The different animal groups had free access to food and water and were kept in a controlled temperature environment (25°C) and 12-h light-dark cycle during the entire experimental period (60 days). All the experiments in this project were approved by the Institutional Committee for Ethics in Animal Experimentation of the University of Campinas (CEUA/UNICAMP; under Protocol: 3439-1).

Weight gain and metabolic evaluation

The following parameters were evaluated in mice from all experimental groups: the weight gain, the visceral (retroperitoneal and pelvic) fat accumulation, the fast and fed glycemia, the fast insulinemia and response to the insulin tolerance test (ITT, expressed as area values under the curve (AUC)). These procedures were performed as previously described[19,40,41] and at the same period during the day (9 a.m.–11 a.m.). The blood glucose concentration was measured using an Accu-Chek Advantage II glucometer (Roche Diagnostic, Switzerland). Insulin plasma concentration was determined using a commercial ELISA kit (Rat/Mouse Insulin ELISA Kit, Cat# EZRMI-13K, Millipore, USA).

Static insulin secretion

Pancreatic islets were isolated from pancreas by collagenase digestion.[41] Groups of five islets of similar size were collected and preincubated in 24-wells plates with 0.5 mL Krebs solution supplemented with 3 mg.mL^{-1} bovine albumin (Sigma) and 5.6 mM glucose for 30 min at 37°C.[40,41] After this period, islet pools were incubated for 60 min at 37°C in Krebs solution supplemented with 2.8 mM or 16.7 mM glucose.[40] After incubation, the supernatants were collected, stored at −20°C until determination of insulin concentration, expressed as ng.mL^{-1}.islet^{-1} using the ELISA kit (Rat/Mouse Insulin ELISA Kit, Cat# EZRMI-13 K, Millipore, USA).

Pancreas and liver histology and morphometry

Pancreas fragments were fixed, embedded in Paraplast® (P3558, Sigma), and routinely processed for hematoxylin–eosin (HE) staining or for immunoperoxidase detection of

insulin.[40] To determine the relative volume of pancreatic beta cells per pancreas, a morphometric analysis was performed as previously described.[40] Briefly, six histological sections from each animal (two sections per pancreas region, i.e. head, body, and tail) were photographed using a digital camera coupled to a conventional inverted microscope (Nikon Eclipse E-400 – Nikon, Japan). The relative volume of beta cells in the pancreas (as an estimate of beta cell mass) was determined by the sum of all insulin immunostained-islet areas divided by the respective pancreas section area using the software ImageJ (http://rsbweb.nih.gov/ij/download.html).

For the analysis of islet cytoarchitecture (i.e. the typical arrangement of beta- and non-beta-cells within the islet),[42] the pancreas sections were processed for dual immunofluorescence for insulin (using the anti-insulin, cat number A0564, Dako, USA) and glucagon (using the anti-glucagon, cat number A0565, Dako, USA) using a standard protocol[19,40] and observed by confocal laser microscopy (LSM 510-Zeiss, Germany).

For the evaluation of adipocyte infiltration within the pancreas, we have used the same histological sections processed previously for HE staining and insulin immunoperoxidase (totalizing 29 pancreas sections/group; 4–5 animals/group). Each pancreas section was scored according to the amount of intralobular fat tissue as follows: score 0, absence of intralobular adipose tissue; score 1, low fat accumulation (presence of one to three adipocytes within pancreas parenchyma section); score 2, moderate fat accumulation (presence of four to six adipocytes within pancreas parenchyma section); score 3, high fat accumulation (presence of more than seven adipocytes within pancreas parenchyma section). The degree of fat accumulation within the pancreas parenchyma was determined by calculating the score mean value for each experimental group according to this classification.

For the analysis of liver steatosis, liver fragments were fixed, embedded in Paraplast® (P3558, Sigma), and routinely processed for HE staining. Digital images (five per liver section) were acquired randomly from three 5-μm-thick sections per liver specimens using a digital camera coupled to a conventional microscope (Nikon Eclipse E-400 – Nikon, Japan). The morphometric estimation of liver steatosis was performed by a point-counting system, as previously described with some modifications,[43] using digital images obtained at high magnification (100 × objective lens) and a test system of 88 points employing the Grid plugin of Image J. The sum of points hitting fat droplets within the hepatocyte was divided by the total points and expressed as percentage that was taken as an index of liver steatosis degree.

Immunolabelling and immunoblotting of claudin-1 in intestine fragments

The localization and distribution of the tight junctional protein claudin-1 in intestinal epithelia were determined by indirect immunofluorescence in cryosections of intestine fragments. For that, fragments of jejunum, ileum, and colon, obtained from 12-h fasted mice were frozen in *n*-hexane with liquid nitrogen and the cryosections obtained were permeabilized and fixed with acetone at −20°C for 3 min. For the immunofluorescence reaction, intestine cryosections were incubated with a blocking solution (phosphate-buffered saline (0.01 mM PBS, pH 7.4) containing 5% bovine serum albumin (BSA) plus 0.1% Tween 20) for 1 h and, then, incubated overnight at 4°C with the anti-claudin-1 primary antibody (Abcam; cat number ab15098; diluted 1:50 in PBS plus 3% BSA). After washing with PBS, the intestine sections were incubated with the FITC-conjugated specific secondary antibody (Sigma) (dilution 1:100 in PBS plus 1% BSA solution) and DAPI (D 9542 Sigma) (dilution 1:1000) for 2 h at room temperature (RT). All sections were mounted in a commercial antifading agent (Vectashield, Vector Laboratories, Burlingame, CA) and photographed by a digital camera coupled to an inverted fluorescence microscope (Observer.Z1; Zeiss – AxioCam, MRC, USA). Digital images of the intestine sections from all experimental groups were obtained and compared during the same session using identical microscope parameters (gain and time exposure). To determine the junctional content of claudin-1 in epithelia from the different intestine segments, five images of intestinal epithelium were captured from each cryosection from animals of all experimental groups. Then, the integrated densities of 50 points per image, placed at the intercellular region of enterocytes (immunolabelled for claudin-1), were measured in all captured images using the free software ImageJ (given a total of 1250 points sampled per experimental group).

Fragments of jejunum, ileum, and colon, where the serosal and muscular layers were removed, were sonicated in an antiprotease cocktail (10 mM imidazole, pH 7.4, 4 mM EDTA, 1 mM EGTA, 0.5 $\mu g.mL^{-1}$ pepstatin A, 200 $KIU.mL^{-1}$ aprotinin, 2.5 $\mu g.mL^{-1}$ leupeptin, 30 $\mu g.mL^{-1}$ trypsin inhibitor, 200 μM DL-dithiothreitol, DTT, and 200 μM phenylmethylsulfonylfluoride (PMSF); Sigma) and processed for Western Blotting, using a standard protocol.[20,41] Briefly, homogenate aliquots (containing 50 μg of total protein) were applied on 12% polyacrylamide gels and proteins were fractionated by electrophoresis and electrophoretically transferred to nitrocellulose membranes (Bio-Rad). After staining with Ponceau solution (Sigma) to check the efficiency of sample loading and transfer, membranes were blocked for 4 h at RT with a buffer solution (0.01 M Trisma Base, 0.15 M NaCl, 0.05% Tween 20; pH 7.4) containing 5% skimmed milk powder and then incubated overnight at 4°C with primary antibody anti-claudin-1 (Abcam; cat number ab15098; dilution 1:150 in basal solution containing 3% skimmed milk powder). After washing with the buffer solution, the membranes were incubated with specific secondary antibody conjugated with HRP (Sigma) (dilution 1:500 in the buffer solution containing 1% skimmed milk powder) for 2 h at RT. Immunoreactive bands were detected using an enhanced chemiluminescence kit (Super Signal, Thermo Fisher Scientific, USA) and an imaging system (Genome Gene, Syngene Bio Imaging, UK). The relative size of the immunoreactive bands was quantified by densitometry using the ImageJ software. After stripping, the membranes were reincubated

with an anti-beta-actin antibody, used as internal control. Optical densitometric values were expressed as the ratio of the claudin-1 and beta-actin signals.

Intestinal permeability to FITC-dextran

Intestinal permeability was assessed by using fluorescein isothiocyanate-conjugated Dextran (FITC-Dextran, 4 kDa, (cat number 46944, Sigma, USA)) as a paracellular tracer.[22] Animals fasted for 6 h received by gavage FITC-Dextran (FITC-DX) solution at a dose of 600 mg.kg^{-1} and volume of 4.8 mL.kg^{-1} (diluted in PBS (0.01 M pH7.4)). After 1 h, the animals were euthanized in a CO_2 chamber; blood samples were collected from the cervical veins (after decapitation) and centrifuged at a speed of 8000*g* for 10 min at 4°C to separate the plasma. Then, plasma aliquots were diluted in an equal volume of PBS (pH 7.4), added to 96-wells plate and read by a fluorescence microplate reader (Fluorskan Ascent; Thermo Scientific, USA) at the excitation wavelength of 485 nm and the emission wavelength of 535 nm. The values of intestinal permeability to FITC-DX were expressed as absorbance absolute values of the marker within the animal plasma.

Statistical analysis

The two-way ANOVA was used to assess the interaction between the two treatments, exposure to butyrate and the HF diet, followed by the Bonferroni post-test. For multiple comparisons, we used the one-way ANOVA, followed by the Bonferroni post-test. In the case of insulin secretory response data, the Student's *t*-test was employed to determine the degree of statistical significance between two experimental groups. All statistical analyses were performed using the GraphPad Prism Software version 5.00 (GraphPad Software, USA). Results are expressed as means + SE (Standard Error), and the significance level was set at $P < 0.05$.

Results

The exposure to HF diet (HF group) for 60 days induced a significant increase in body weight gain (of 35.8%) ($P < 0.001$) (Figure 1(a)) and in visceral adipose tissue deposition (of 6.3 fold) ($P < 0.0001$) (Figure 1(b)) as compared to control (C) group. HF diet also induced metabolic disturbances that included, marked peripheral insulin resistance ($P < 0.05$) (Figure 1(c) and (d)), significant fast ($P < 0.0001$) and fed ($P < 0.0001$) hyperglycemia (Figure 1(e) and (f)) as well as fast hyperinsulinemia ($P < 0.05$) (Figure 1(g)). Interestingly, diet supplementation with 5% sodium butyrate (HFB group) significantly reduced the adiposity and all metabolic alterations induced by HF diet. Butyrate treatment blocked completely the development of insulin resistance and hyperinsulinemia states induced by HF diet (Figure 1(d) and (g)). Mice from HFB group displayed a significant decrease of 50.5% in body weight gain, 27.7% in adipose tissue accumulation, and 19.7% and 15.9% in fast and fed hyperglycemia, respectively, as compared to those from HF group (Figure 1). In addition, butyrate *per se* (CB group) has no adverse effects on the parameters evaluated as compared to the control group (Figure 1).

In order to confirm that the protective effect of sodium butyrate on the parameters studied was not a result of differences in diet ingestion, we have monitored the daily food consumption in all experimental groups throughout the experimental procedure. The food intake values expressed in kcal confirm that there was no significant difference in kcal intake between HF and HFB groups (Figure 1(h)). In addition, the food consumption in grams was similar among the different treatments (C 6.04 ± 0.16 g; HF 6.35 ± 0.08 g; CB 5.19 ± 0.18 g; HFB 6.05 ± 0.09 g ($n = 18$)).

It is well known that the insulin resistance state in T2DM can result in structural adaptations of the endocrine pancreas and functional defects in the insulin-secreting pancreatic beta cells.[15–19] To investigate whether supplementation with sodium butyrate has also an effect on insulin secretion, batches of isolated pancreatic islets from mice of all experimental groups were *in vitro* exposed to 2.8 mM or 16.7 mM glucose for 60 min (Figure 2). At basal condition (2.8 mM glucose), islets isolated from mice of the HF group showed a significant increase in basal insulin release as compared to control group (Figure 2(a)), which is in agreement with our previous data.[20,41] Interestingly, this increased basal secretion was not observed in islets from mice receiving diet supplementation with butyrate (HFB group) (Figure 2(a)). At stimulated condition (when exposed to 16.7 mM glucose), the release of insulin by islets isolated from HF-fed mice group was similar to that by control islets (Figure 2(b)). Comparatively, islets from mice receiving supplementation with butyrate (CB and HFB groups) displayed a tendency of an increase, although not statistically significant, in insulin secretion at the supraliminal concentration of glucose (16.7 mM) (Figure 2(b)). This change resulted in a significantly higher ($P = 0.012$) fold increase in glucose-induced insulin secretion in HFB islets (56.5 ± 18.8 (10) fold as compared to basal secretion) than HF islets (10.5 ± 3.4 (13) fold as compared to basal secretion), which, in turn, displayed a significant lower ($P = 0.02$) secretory response to glucose as compared to control (C) islets (32.4 ± 7.9 (14) fold as compared to basal secretion).

In accordance with our previous data,[19,20,41] 60 days of exposure to HF diet induced a compensatory beta cell mass expansion as revealed by the significant increase in the relative volume of beta cells in relation to the total pancreas (Figure 3(b) and (e)) as compared to controls (Figure 3(a) and (e)). This was accompanied by no changes in islet cytoarchitecture, characterized by a core of insulin-secreting beta cells surrounded by a peripheral mantle of glucagon-secreting alpha cells in HF mice, which was verified in all other experimental groups (C, CB, HFB) (Figure 3(f) to (i)). Interestingly, the compensatory beta cell mass expansion was not observed in the groups that received supplementation with sodium butyrate (HFB and CB) (Figure 3(c) to (e)).

Considering the protective effect of sodium butyrate against the HF diet-induced adiposity and disturbance of the beta cell insulin secretion, we also evaluated the degree of lipid accumulation in the liver and adipocyte infiltration

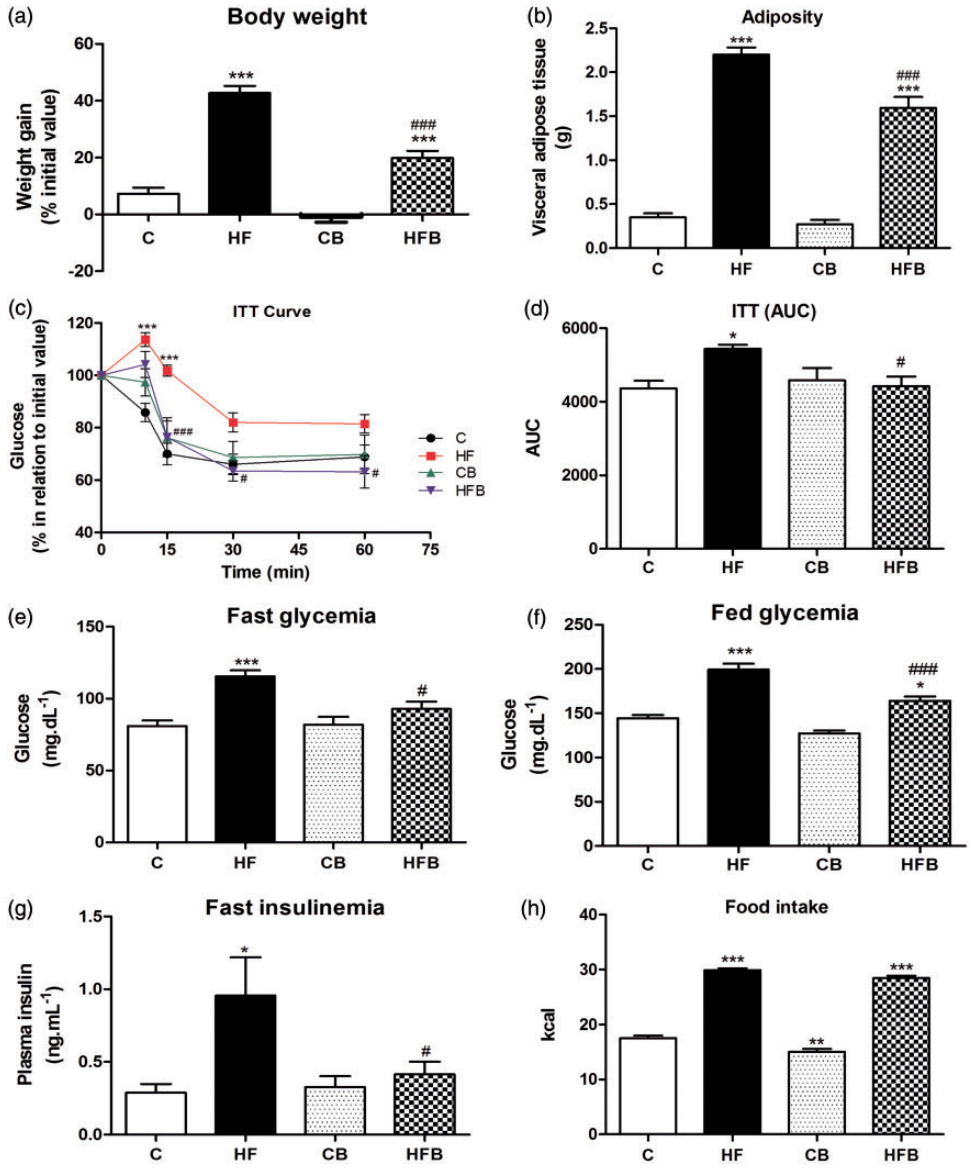

Figure 1 Butyrate treatment significantly reduced the high-fat diet-induced obesity and metabolic dysfunctions in mice without changing food intake. As compared to control group, high-fat (HF) diet for 60 days induced a significant increase in weight gain (a), adiposity (b), in peripheral insulin resistance (c), as assessed by the insulin tolerance test (ITT) and expressed as area values under the curve (AUC) (d), in fast (e) and fed (f) glycemia and in fast insulinemia (g), suggesting the development of prediabetes in these mice. However, dietary supplementation with 5% sodium butyrate (HFB group) showed a protective effect reducing significantly all these metabolic alterations induced by HF diet, without changing the food intake expressed as calories (h). Administration of butyrate *per se* (CB) did not significantly affect the parameters evaluated as compared to control group (C). Data are expressed as means + SE of at least three independent experiments ($n = 14$–18 mice per group). Groups: C = control (fed a regular diet alone); HF: high-fat diet alone; CB: Control + butyrate; HFB: high-fat diet + butyrate.*$P < 0.05$, **$P < 0.001$, ***$P < 0.0001$ compared to C group. #$P < 0.05$, ###$P < 0.0001$ compared to HF group. (A color version of this figure is available in the online journal.)

in the pancreas in all experimental groups studied (Figure 4). As compared to C group, exposure to HF diet induces a significant accumulation of fat in the liver (21.3% of total liver volume), which was characterized by the presence of large- and medium-sized lipid droplets within hepatocytes cytoplasm (macrovesicular steatosis) (Figure 4(e)). Supplementation with sodium butyrate resulted in a significant reduction in hepatic steatosis (11.3% of total liver volume) (Figure 4(e)) ($P < 0.0001$), where hepatocytes of HFB mice displayed mainly a single small-sized lipid droplet or multiple lipid vesicles of very small size in their cytoplasm (Figure 4(d)). No evidence of hepatic lipid accumulation was observed in the control groups, receiving or not butyrate (C and CB) (Figure 4(a) and (c)). In addition, adipocyte infiltration was observed in the pancreas of animals exposed to HF diet (Figure 4(g) and (j)) as compared to the C group (Figure 4(f) and (j)). In HF diet-fed mice that received diet supplementation with sodium butyrate, there was a significant decrease in the intrapancreatic deposition of adipose tissue (Figure 4(i) and (j)) as well as a reduction in adipocyte size as compared to the pancreas from HF group (Figure 4(g) and (j)). In contrast, the amount of intrapancreatic adipose tissue was negligible in the control groups (C and CB) (Figure 4(f), (h) and (j)).

Considering the protective effect of butyrate on the metabolic parameters studied, as well as on the reduction of the

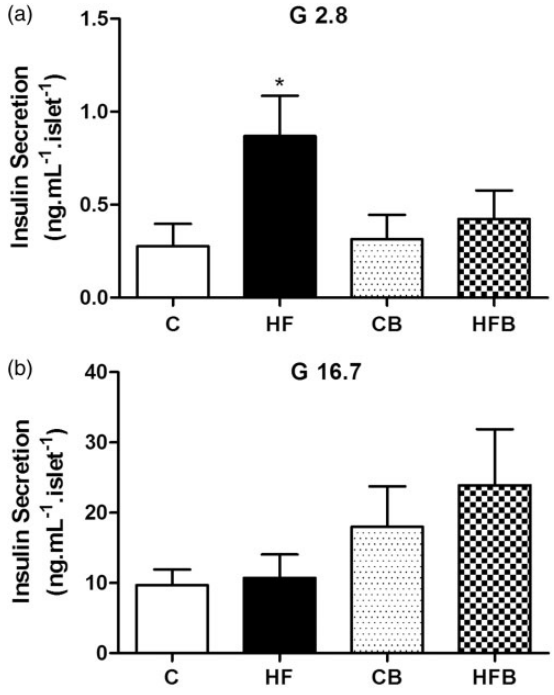

Figure 2 Pancreatic islets from high fat-fed mice show altered insulin secretion that was not observed after treatment with butyrate. Batches of isolated islets from mice of all experimental groups were exposed to 2.8 (a) or 16.7 mM glucose (b) for 60 min. Compared to controls (C), islets from HF-fed mice (HF) showed increased basal insulin secretion (expressed as ng.mL^{-1}.islet^{-1}) in the presence of 2.8 mM glucose (G 2.8) but a comparable insulin release when stimulated by 16.7 mM glucose (G 16.7) (b). This increased basal secretion was not observed in HF-fed mice receiving diet supplementation with butyrate (HFB) as compared to its control (CB)(a); but a tendency of an increase in stimulated insulin release (b) was verified in mice with butyrate diet supplementation (CB and HFD groups) as compared to those not receiving this SCFA (C and HF groups). Bars represent means + SE of four independent experiments (10–14 batches of five islets isolated from four mice per group). *$P < 0.05$ compared to C group

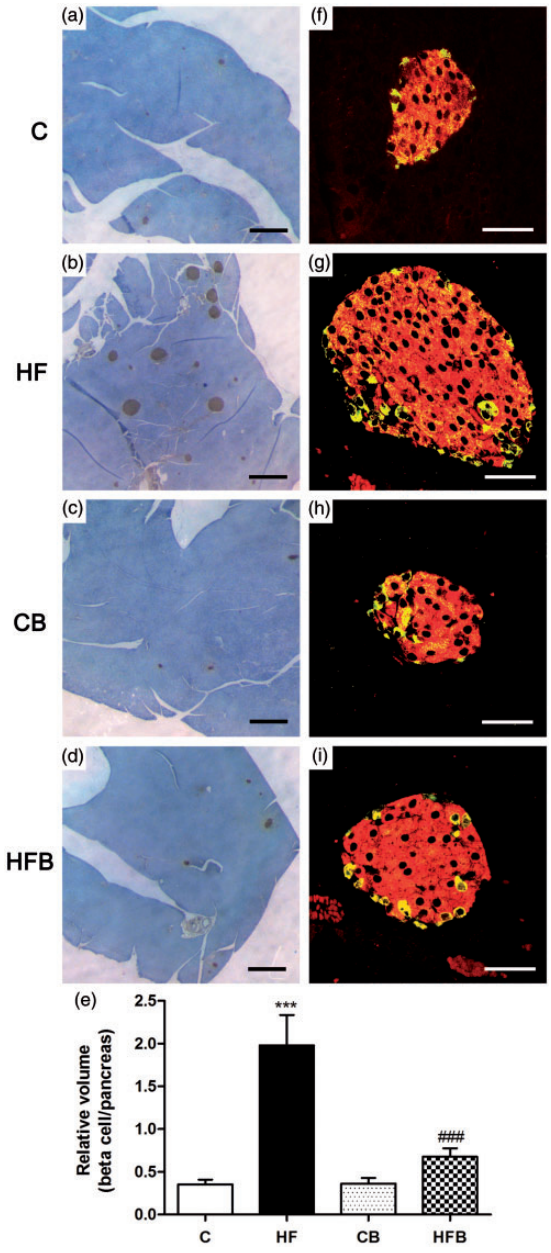

Figure 3 The compensatory beta cell mass expansion induced by high-fat diet in mice was not observed after butyrate administration. Photomicrographs of pancreatic islets processed for insulin immunoperoxidase (a–d) (brown) or for double immunofluorescence to detect insulin (red) and glucagon (yellow)(f–i). Note the increase in number and size of insulin-labelled islets (b,g), with no change in the islet cytoarchitecture (g), in high-fat diet-fed mice (HF) in comparison with control group (C) (a,f). This increase in the relative volume of insulin-producing beta cells induced by HF diet was not observed after butyrate treatment (HFB) (d,i) as compared to its control (CB) (c,h); this result was confirmed quantitatively as shown in (e). Bars in graph (e) represent means + SE of six mice per group. Images were obtained by light (a–d) or confocal laser microscopy (f–i). Scale bars, 500 μm in (a–d); 50 μm in (f–i). ***$P < 0.0001$ compared to C group; ###$P < 0.0001$ compared to HF group. (A color version of this figure is available in the online journal.)

accumulation of lipids within organs directly related to the insulin body response, we evaluated whether there was a concomitant effect of butyrate on the intestinal epithelial barrier. The evaluation of the intestinal epithelial barrier by claudin-1 immunodetection in intestinal cryosections showed a significant decrease in the intercellular content of this TJ-associated protein in enterocytes of HF-fed mice, in all studied intestinal segments ((jejunum (reduction of 26.4%) (Figure 5(c) and (e)), ileum (of 25.6%) (Figure 5(c) and (e)) and colon (of 19.4%) (Figure 6(c) and (e))) as compared to that observed in the C group, suggesting an impairment of the structure of the intestinal epithelial barrier after HF diet treatment. Supplementation with sodium butyrate reversed this alteration by inducing a significant increase in the degree of junctional content of claudin-1 within intestinal epithelia (jejunum (increase of 46.4%) (Figure 5(d) and (e)), ileum (34.3%) (Figure 5(d) and (e)) and colon (66.1%) (Figure 6(d) and (e)) in comparison with that observed in the HF group. Besides the increased intercellular content, we consistently observed a higher labeling for claudin-1 at enterocyte cytoplasm of intestine fragments from mice treated with butyrate, which suggested increased protein expression. However, the immunoblotting analyses showed no significant change in total protein content of claudin-1 in intestinal fragment homogenates among the differents experimental groups. Nevertheless, we observed a tendency of a decrease in claudin-1 protein content in HF group as compared to C group as well as a tendency of increase in claudin-1 protein content in the groups receiving

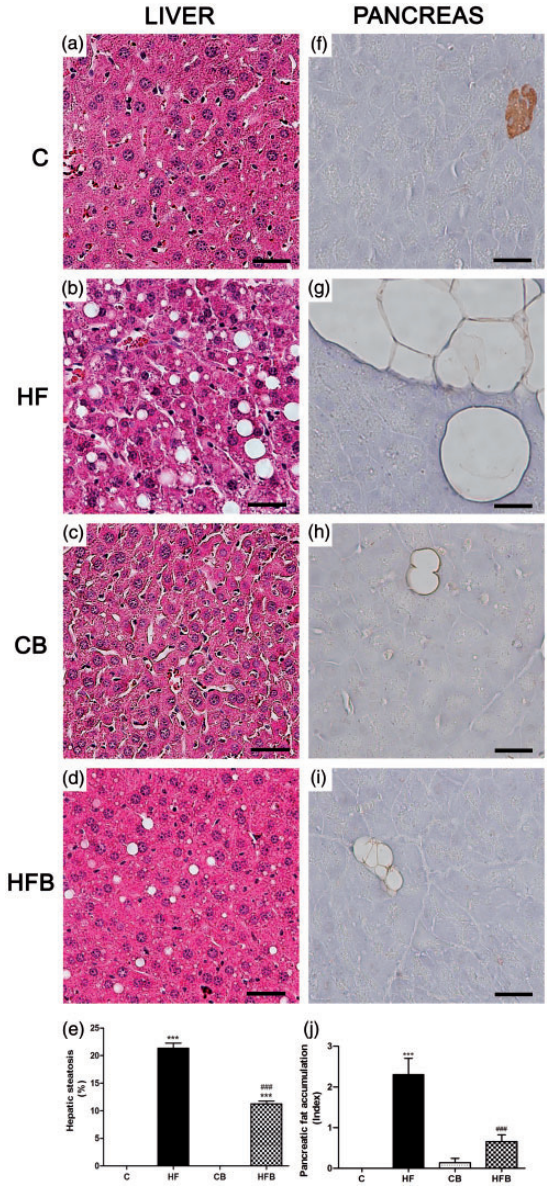

Figure 4 Diet supplementation with butyrate inhibited hepatic steatosis and pancreatic fat accumulation induced by high-fat diet in mice. Photomicrographs of the liver (a–d) routinely processed for HE staining and pancreas processed for insulin immunoperoxidase (brown) (f–i). Exposure to high-fat (HF) diet-induced liver steatosis (b,e) and pancreatic fat accumulation (g,j) in HF mice as compared to controls (C) (a,f,e,j) that were significantly reduced by administration of butyrate (HFB) (d,i,e,j). No significant changes were observed with butyrate *per* se (CB group) (c,h) in comparison with C group (a,f). Scale bars, 50 μm. $^{***}P < 0.0001$ compared to C group ; $^{###}P < 0.0001$ compared to HF group. (A color version of this figure is available in the online journal.)

supplementation with sodium butyrate (Figures 5 and 6). A possible explanation for the apparent discrepancy between the immunofluorescence and immunoblotting data is that, in the case of immunofluorescence, measurements of claudin-1 junctional content were made exclusively in the region of the epithelium, that highly express this protein, while the evaluation of the total cell content by Western Blot was done in homogenates of intestinal fragments that contain not only the epithelium but other tissues (particularly the connective layer of the lamina propria and submucosa) that make up the intestinal wall. The presence of these tissues, where the expression of TJ proteins is low or non-existent, may interfere with the sensitivity of the immunoblotting method to detect subtle differences in the expression of these proteins in the epithelium, as probably happened in our experiments.

Taken into account the marked increase in claudin-1 immunodetection seen in intestinal epithelial cryosections of butyrate-treated mice in comparison with controls, we performed a functional analysis of the intestinal epithelial barrier using the FITC-Dextran (FITC-DX) permeability test. This analysis revealed that CB (Abs DX-FITC $0.61 \pm 0.15(6)$) and HFB mice (Abs DX-FITC $0.47 \pm 0.13(6)$) showed a significant decrease in intestinal absorption of the paracellular marker compared to control (C) group (Abs DX-FITC $2.1 \pm 0.55(6)$) ($P < 0.05$), which was in agreement with the immunofluorescence data.

Discussion

Type 2 diabetes (T2DM) associated with obesity is reaching worldwide epidemic proportions.[1,4,5] Therefore, there is an increasing interest in understanding thoroughly the T2DM pathogenesis in order to find new strategies for treatment and prevention of this disorder. The central feature of the T2DM is the development of a body resistance to insulin that is characterized by a reduction in tissue response/sensitivity (particularly of muscle, adipose, and hepatic tissues) to this hormone and, as consequence, a chronic state of hyperglycemia develops.[6–8,44] It has been recently suggested that consumption of lipid-enriched diet results in disruption of the intestinal epithelial barrier, allowing the passage of noxious agents leading, in turn, to a systemic inflammatory response that could be a primary cause of the peripheral insulin resistance.[12,22,24–28,45] Recent works have focused on changes in microbiota and in luminal content composition as a result of HF diet consumption and its relation to intestinal barrier disruption, local/systemic immune response and/or insulin resistance state in T1DM and T2DM diabetes.[12,46–48] These studies have opened a new perspective of investigation aiming at the use of probiotics, prebiotics, and postbiotics (such as SCFAs) as adjunctive therapy of diabetes.[24,28,29,31,38,49] Some studies have demonstrated that sodium butyrate, a SCFA, has beneficial effects on animal models of T1DM and T2DM.[31,36,39] In the present work, we demonstrated that butyrate alleviates the metabolic impairments induced by HF diet administration in mice, by inhibiting the development of an insulin resistance state, which was associated with improvement of insulin-secreting function of beta cells and strengthening of the TJ-mediated intestinal epithelial barrier.

Confirming our previous works,[19,20,41] we described herein that the exposure to a diet with high content of lipids (21% w/w, corresponding to 45% of fat in calories) for only 60 days induced, in C57 mice, obesity and prediabetes, which were characterized by a significant body adiposity, marked insulin resistance associated with moderate hyperglycemia and significant hyperinsulinemia. The treatment with sodium butyrate prevented all these HF diet-induced alterations, which cannot be attributed to

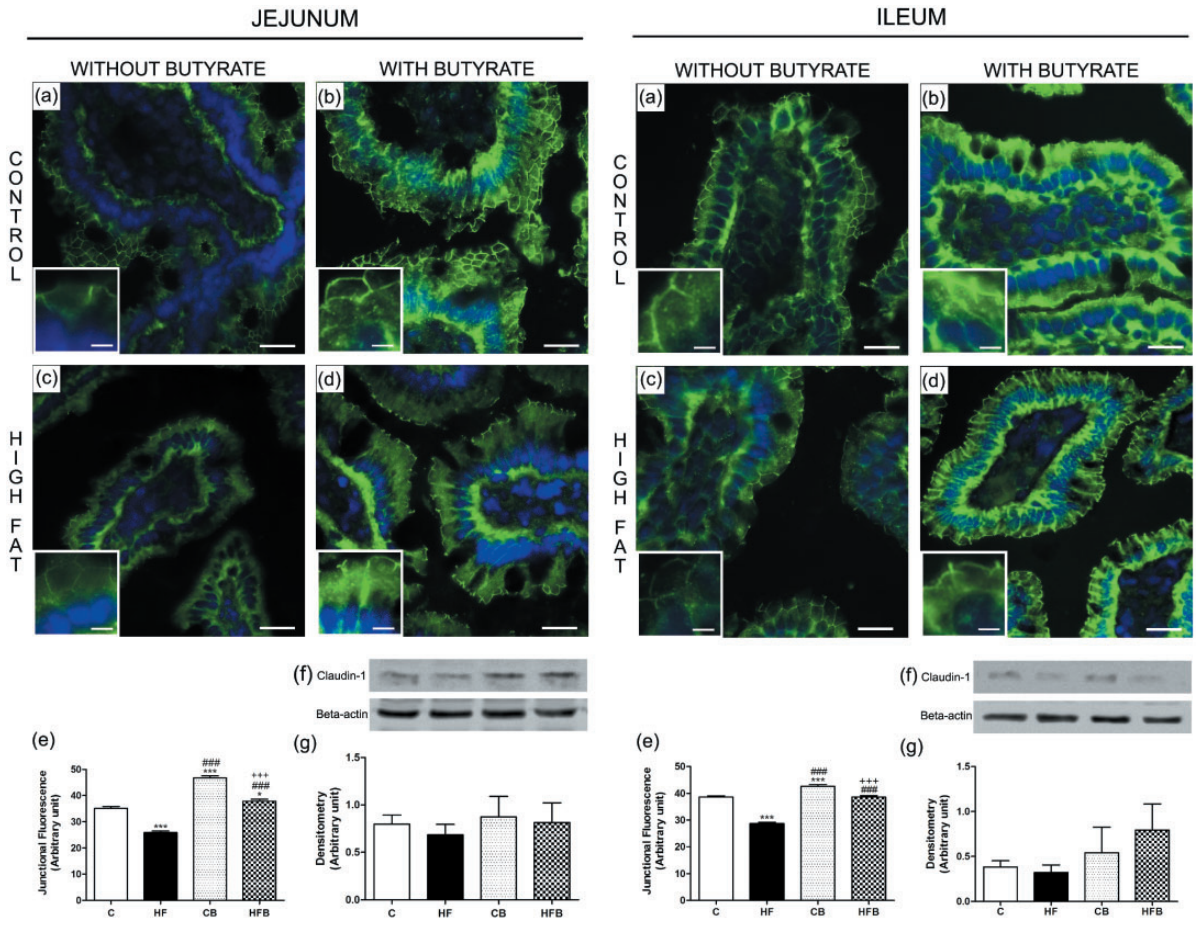

Figure 5 Butyrate, given as dietary supplementation, increased the junctional content of claudin-1, a tight junction-associated protein, in intestinal epithelia of the small intestine (jejunum and ileum). The junctional and total cell contents of claudin-1 were evaluated by immunofluorescence in intestinal cryosections (claudin-1 in green; DAPI/nuclei in blue) and by Western Blot in intestine homogenates, respectively. The analysis of the degree of fluorescence at the cell-cell contact showed a significant decrease in the intercellular content of claudin-1 in enterocytes of small intestine from HF diet-fed mice (HF group)(c,e), which was inhibited by the administration of butyrate to treated animals (HFB group) (d,e). The total cell content of this junctional protein displayed no significant changes after HF diet and/or butyrate treatment as revealed by immunoblotting (f,g). Groups: C: control (fed a regular diet alone); HF: high-fat diet alone; CB: control + butyrate; HFB: high-fat diet + butyrate. Scale bars, 15 μm (insets); 50 μm (images a–d).*$P < 0.05$, ***$P < 0.0001$ compared to C group, $^{\#\#\#}P < 0.0001$ compared to HF group,$^{+++}P < 0.0001$ compared to CB group. (A color version of this figure is available in the online journal.)

differences in food intake since diet consumption in calories was similar between the HF and HFB groups. Gao *et al.*,[39] employing a comparable animal model of T2DM (mice fed a HF diet containing 58% of fat in calories for up to 16 weeks), have shown similar results with butyrate. They suggested that the anti-obesity effect of butyrate is a result of an increase in body energy expenditure, induction of mitochondria function and fatty acid oxidation, which were mediated by the activation of PGC-1α in brown adipose and skeletal muscle tissues.[39] However, their study lacked the control groups (receiving a regular chow diet with or without supplementation with butyrate) which made it difficult to establish the effectiveness of the butyrate treatment in reaching control values regarding the parameters evaluated in HF diet-fed mice, as well as it did not investigate the metabolic effects of this SCFA *per se.* This was overcome in our study that interestingly showed that diet supplementation with butyrate completely blocked the development of the insulin resistance state in these HF diet-fed mice, that displayed a sensitivity to insulin similar to control values, as revealed by ITT analysis. In addition, butyrate treatment significantly reduced the body weight gain (in 50%), the visceral adipose tissue accumulation (in 28%) and hyperglycemia at fast (in 16%), and fed (in 20%) conditions after HF diet exposure when compared to the group that did not received this SCFA (HF group). However, in contrast to the response to ITT, the adiposity and glycemia of animals from HFB group did not reach control levels after butyrate. In addition, we showed that butyrate treatment *per se* did not affect markedly body weight and metabolic parameters in mice fed a regular diet, indicating that this SCFA acts mainly when animal metabolism is challenged by a modified diet.

One of the consequences of consumption of HF diet is the development of a fatty liver, a condition known as hepatic steatosis.[50] Hepatic steatosis is closely related to obesity, insulin resistance state, and T2DM, and, although it is reversible, can aggravate the metabolic disturbances associated with these disorders or evolved to a more serious condition known as non-alcoholic steatohepatitis

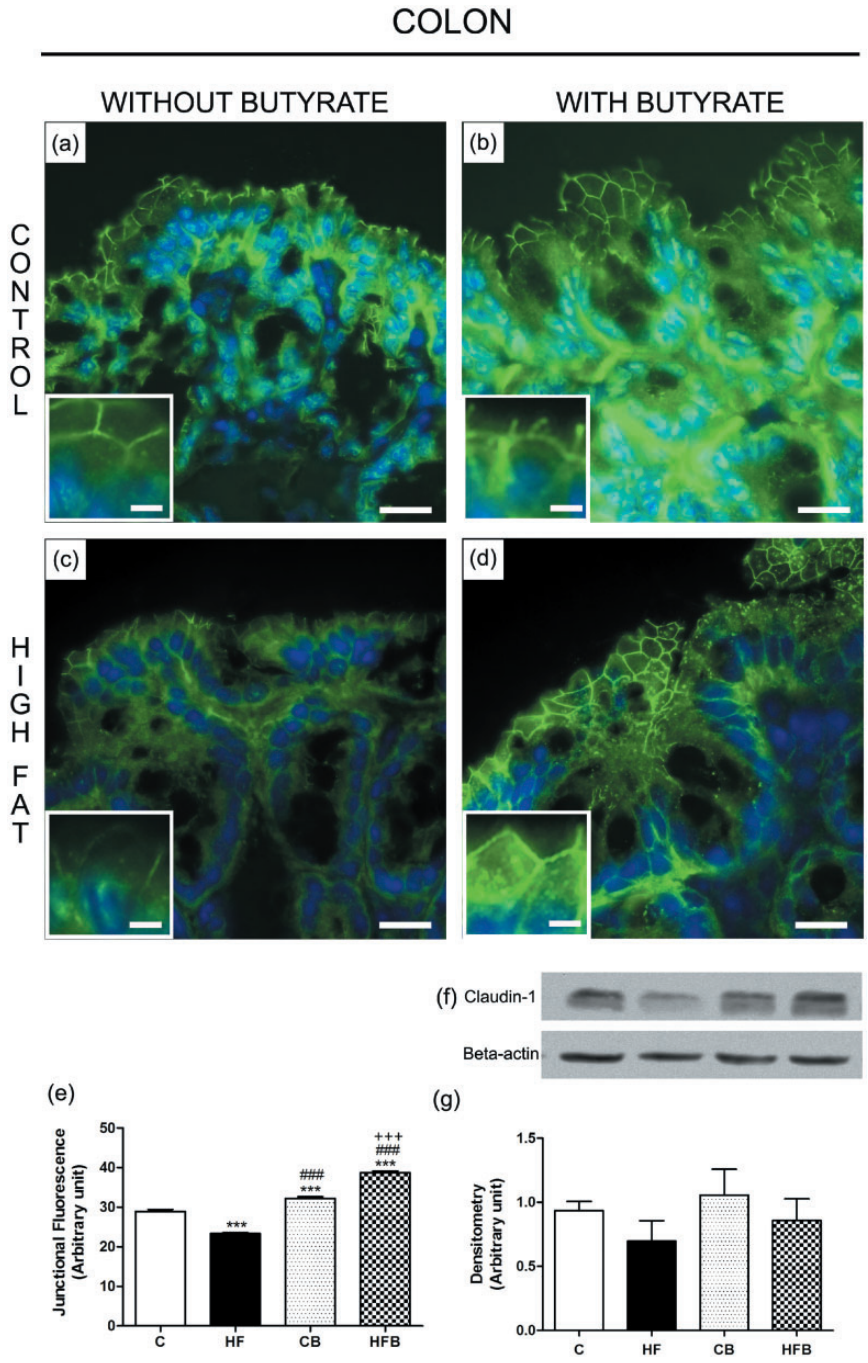

Figure 6 Butyrate inhibited the reduction in the junctional content of claudin-1 in enterocytes of the large intestine (colon) induced by exposure to the high-fat diet in mice. The junctional and total cell contents of claudin-1 were evaluated by immunofluorescence in colon cryosections (claudin-1 in green; DAPI/nuclei in blue) and by Western Blot in colon homogenates, respectively. The analysis of the degree of fluorescence at the cell–cell contact showed a significant decrease in the intercellular content of claudin-1 in enterocytes of colon from HF diet-fed mice (HF group)(c,e) as compared to controls (C group) (a,e); this was inhibited by the administration of butyrate to treated animals (HFB group) (d,e). The total cell content of this junctional protein displayed no significant changes after HF diet and/or butyrate treatment as revealed by immunoblotting (f,g). Groups: C: control (fed a regular diet alone); HF: high-fat diet alone; CB: control + butyrate; HFB: high-fat diet + butyrate. Scale bars, 15 μm (insets); 50 μm (images a–d). $^{***}P < 0.0001$ compared to the C group, $^{###}P < 0.0001$ compared to HF group, $^{+++}P < 0.0001$ compared to CB group. (A color version of this figure is available in the online journal.)

(NASH).[50–52] In our study, we investigated whether butyrate could revert a possible hepatic steatosis in our animal model. Firstly, as revealed by morphometric analysis, we showed that 60 days of exposure to HF diet resulted in the appearance of lipid-containing hepatocytes representing approximately 21% of total liver volume, that typically characterizes a hepatic steatosis state (clinically defined as the accumulation of lipids in at least 5% of hepatocytes).[51] Interestingly, the diet supplementation with butyrate reduced significantly the hepatic steatosis in HF diet-fed mice by decreasing not only the number of hepatocytes affected (to only 11% of total liver volume) but also the

size and frequency of cytoplasmic lipid droplets. In agreement with our data, Khan and Jena[35] have recently shown that butyrate decreased the fat accumulation in the liver in streptozotocin-induced diabetic rats fed a HF diet, although they did not analyze these data morphometrically but only qualitatively. It has been proposed that the accumulation of triglycerides (TG)-based lipid droplets within hepatocyte cytosol is result of one or a combination of the following mechanisms: (1) increased uptake of free fatty acids (FFAs) from HF food and of those released by adipocytes at IR condition (where lipolysis is upregulated); (2) increased *de novo* synthesis of FFAs in the liver from glucose or acetate by IR; (3) decreased hepatic mitochondrial β-oxidation of FFAs; and (4) decreased clearance of TG by VLDL particles from the liver.[50–52] Therefore, the inhibitory effect of butyrate on high fat diet-induced hepatic steatosis reported by us may reside from the fact that at least three of these mechanisms (identified as 1, 2 and 3) could be potentially reversed by this SCFA treatment as result of its beneficial action on glucose homeostasis, peripheral insulin sensitivity, FFA oxidation and mitochondrial function as documented herein and by others.[39]

It is well known that the pancreatic beta cell plays a central role in the T2DM pathogenesis, displaying an adaptive response in order to compensate the resistance of peripheral tissues to insulin.[5,16–19] For that, beta cells initially enhance the biosynthesis and release of this hormone followed by an increment of beta-cell mass by hypertrophy and/or hyperplasia. When the beta cells fail to maintain the normoglycemia, T2DM is triggered, resulting in insulin secretory impairment and then beta-cell death by apoptosis at advanced stages, which leads to an irreversible body dependence on exogenous insulin. In our animal model of prediabetes, we observed an increased release of insulin at basal glucose concentration (2.8 mM) by pancreatic islets isolated from HF diet-fed mice as compared to controls, which agrees with our previous works.[20,41] Increased basal insulin secretion is one of the features of the early phase of T2DM in human[53,54] and rodents[55,56] and it has been associated with an aggravation of the insulin resistance state and glycemia dysregulation. Interestingly, we demonstrated that butyrate diet supplementation prevented this condition in HFB islets, which displayed a basal insulin release level similar to control islets (C and CB groups). In addition, we observed a tendency of an increase in stimulated insulin secretion (at 16.7 mM glucose) in CB and HFB islets. As a consequence, butyrate treatment led to a significant improvement of the glucose-induced secretory response of beta cells, assessed as fold stimulation at 16.7 mM over that at 2.8 mM glucose exposure, i.e. HFB islets displayed a 56-fold increase in contrast with the 10-fold increase in glucose-stimulated insulin secretion observed in HF islets. To the best of our knowledge, this is the first study reporting a positive effect of this SCFA on insulin secretion in isolated islets. However, the mechanism involved in this phenomenon is still unknown as also is our knowledge very limited on the cellular processes underlying the changes in basal insulin secretion during T2DM. Nagaraj *et al.*[57] have recently proposed that the reduced presence of cholesterol-enriched membrane rafts in beta cells, that well known determine the spatial organization of the exocytosis-related SNARE proteins and K^+ and Ca^{2+} channels, could contribute to the elevated basal insulin secretion seen in type 2 diabetes. Interestingly, they also showed that prolonged high glucose exposure (up to 72 h) decreased membrane rafts in a beta cell lineage in culture, suggesting that hyperglycemia could be involved in the phenomenon.[57] Therefore, the general protective action of butyrate on glucose homeostasis after HF diet challenge may explain, at least partially, the effect of this SCFA on insulin secretion at cellular level. Additionally, Pinnick *et al.*[58] have suggested that changes in the fatty acid milieu of the islet, as result of adipocyte infiltration in pancreatic exocrine tissue associated with HF feeding in mice and with type 2 diabetes in humans, can be deleterious to islet secretory function. Taken this into consideration, the fact that butyrate-treated mice displayed significant lower adipose tissue infiltration within pancreas parenchyma after HF diet exposure, as compared to HF mice, may be another contributing factor.

Our prediabetic mice also displayed a significant beta cell mass expansion, which was not accompanied by changes in islet cytoarchitecture, as compared to control animals. The increase of beta cell mass and basal insulin secretion observed in our HF diet-fed mice corroborates the data showing a significant hyperinsulinemia at a fast condition in these animals. In previous works, we have shown that the increased beta cell mass resulted from beta-cell hypertrophy as well as from self-replication of this cell type, as revealed by Ki67 immunodetection (a marker of cell proliferation).[19,20] In addition, Oliveira *et al.*[19] showed that there is a direct correlation between the degree of beta cell mass expansion and the level of hyperglycemia (mainly at fed state), and insulin resistance in HF diet-fed mice, where the former parameter displayed a higher correlation index ($r = 0.929$) than the latter as assessed by ITT ($r = 0.817$). In the present study, we reported that butyrate treatment significantly reduced the HF diet-induced increase in beta cell mass, which is in line with our findings showing a marked inhibitory effect of this SCFA on postprandial hyperglycemia and insulin resistance state (that was completely blocked).

Besides the endocrine pancreas, the intestinal tract and the associated microbiota have been considered as a pivotal organ for the onset and evolution of both T1DM and T2DM.[22,25,45,59,60] Based on clinical and experimental evidence, the current hypothesis postulates that a disruption of the intestinal epithelial barrier induced by a modified microbiota or altered luminal content would lead to an increased intestinal permeability to antigens from dietary, viral or bacterial origin, that in turn could activate autoimmune reactions against insulin-producing beta cells (in T1DM) and/or elicit secretion of pro-inflammatory cytokines, locally and systemically, leading to insulin resistance (in T2DM).[14,48,61,62] Given our current knowledge, one may assume that reinforcing the intestinal barrier can offer and open new therapeutic horizons in the treatment of these two types of diabetes. Taken all into consideration, we went to investigate the effect of butyrate supplementation on intestinal barrier function in our animal model of T2DM,

focusing on the structure and function of the intestinal TJ, an essential element of this barrier.[62–65]

Exposure to HF diet for 60 days induced a significant decrease in the junctional content of claudin-1, a constitutive protein of intestinal TJ,[63] and a tendency of reduction in total protein content of this protein in the epithelium of intestinal segments (jejunum, ileum and colon), as revealed by immunohistochemistry and Western Blot, respectively. The decrease of the claudin-1 junctional content in the intestinal epithelium observed in our prediabetic mice may be a result of the internalization of this protein from the TJ site to the cytoplasm for degradation, which certainly leads to disruption of TJ function. Similar changes in molecular structure of TJ, associated with increased epithelial permeability to paracellular markers, have been reported *in vitro* system using colonic cell lines exposed to Escherichia coli bST toxin[66] or to pro-inflammatory cytokines IFN-γ and TNF-α.[67] To the best of our knowledge, this is the first report showing changes in the molecular arrangement of TJ in an animal model of T2DM and is in line with works documenting enhancement of intestinal permeability, as revealed by permeability assays with paracellular markers, in type 2 diabetic rodents and humans.[22,45,46,68,69] In addition, exposure to sodium butyrate induced a strengthening of the intestinal epithelial barrier, as revealed by the statistically significant decrease in intestinal permeability to FITC-dextran in CB and HFB groups compared to C group. In accordance with this data, we found that treatment with butyrate resulted in significant increase in immunostaining (both at intercellular and cytoplasmic region) and a tendency to increase the protein content of claudin-1 in the intestinal segments studied. This result is in accordance with the inhibitory effect of this SCFA on the metabolic alterations (particularly the insulin resistance state) induced by HF diet feeding and corroborate the hypothesis suggesting a role of the intestinal tract in the T2DM pathogenesis.

Studies investigating the effect of butyrate on the expression of junctional proteins in epithelium are rare, but overall they are in agreement with a positive action of this agent on TJ function. Wang *et al.*[34] have observed that sodium butyrate induced increase in gene expression and protein content of claudin-1 in the intestinal epithelial cell line IEC, possibly due to a higher level of interaction between the SP1 transcription factor, and its promoter. Additionally, Huang *et al.*[70] reported that the decrease in paracellular intestinal permeability, as measured by lactulose/mannitol assay in urine, is associated with increased expression of occludin in jejunum and colon segments of newborn pigs after butyrate treatment in combination with antibiotics. The authors suggested that this effect on intestinal function was probably due to an anti-inflammatory action of this SCFA since the TNF-α concentration was lower in the mucosa of animals receiving treatment with butyrate.[70]

The mechanism of action of sodium butyrate on cellular expression of claudin-1 or other structural proteins of TJ is still unknown; however, it may also be related to its action as an inhibitor of the HDAC enzyme. Sodium butyrate causes hyperacetylation of histones by inhibiting histone affinity with DNA and thus increases the exposure of regions for transcription of certain genes.[37,71] It is known that proteins associated with intercellular junctions such as connexins (the gap junction proteins), and ZO-1 (a TJ-associated protein) may undergo epigenetic regulation under certain experimental conditions.[72,73] However, future experiments will be necessary to unravel, at the molecular level, how butyrate affects junctional protein expression and/or assembly/disassembly at intestinal TJ in our experimental model of type 2 prediabetes.

In conclusion, our data showed a protective action of butyrate on metabolic, hepatic and pancreatic alterations induced by HF diet in mice. Given the well-known association between obesity and T2DM,[4–6] the improvement of glucose homeostasis and insulin sensitivity in HF-fed mice after butyrate treatment may be related to the inhibitory effect of this SCFA on adiposity as reported herein and to the butyrate-induced increase in energy expenditure as described elsewhere.[39] In addition, the strengthening of the intestinal epithelial barrier associated with butyrate treatment may play a role in the process. A deeper understanding of the molecular pathways involved in the regulation of intestinal barrier and lipid/carbohydrate metabolism by butyrate will have important clinical implications by potentially opening new horizons in the treatment and prevention of diabetes mellitus and related metabolic disorders, as well as of unrelated intestinal diseases.

Authors' contributions: VAM participated in the study conception, conducted the experiments, analysis, and interpretation of data and reviewed the manuscript; LCSM, RBO, DAM conducted the experiments, analysis, and interpretation of data and reviewed the manuscript; CBCB was responsible for the study conception and design of the experiments, critical interpretation of the data, drafting and review of the manuscript.

ACKNOWLEDGMENTS

The authors thank Dr. Valéria Quitete and Dr. Eduardo Galembeck for allowing the access to their laboratory facilities. CBC-B (CNPq # 304991/2015-5) is a recipient of Research Fellowship from Conselho Nacional de Desenvolvimento Científico e Tecnológico (CNPq, Brazil).VAM is a recipient of a PhD fellowship from CAPES (Brazil). This work was funded by grants from FAPESP (2013/15676-0), CAPES and CNPq (Brazil).

DECLARATION OF CONFLICTING INTERESTS

The authors declare that they have no conflict of interest with respect to the research, authorship, and/or publication of this article.

REFERENCES

1. American Diabetes Association. Diagnosis and classification of diabetes mellitus. *Diab Care* 2014;**37**:81–90
2. Thomas CC, Philipson LH. Update on diabetes classification. *Med Clin North Am* 2015;**99**:1–16
3. Canivell S, Gomis R. Diagnosis and classification of autoimmune diabetes mellitus. *Autoimmun Rev* 2014;**13**:403–7

4. Olokoba AB, Obateru OA, Olokoba LB. Type 2 diabetes mellitus: a review of current trends. *Oman Med J* 2012;**27**:269–73
5. Tripathy D, Chavez AO. Defects in insulin secretion and action in the pathogenesis of type 2 diabetes mellitus. *Curr Diab Rep* 2010;**10**:184–91
6. Lee BC, Lee J. Cellular and molecular players in adipose tissue inflammation in the development of obesity-induced insulin resistance. *Biochim Biophys Acta* 2014;**1842**:446–62
7. Björnholm M, Zierath JR. Insulin signal transduction in human skeletal muscle: identifying the defects in Type II diabetes. *Biochem Soc Trans* 2005;**33**:354–7
8. Wilcox G. Insulin and insulin resistance. *Clin Biochem Rev* 2005;**26**:19–39
9. Forbes JM, Cooper ME. Mechanisms of diabetic complications. *Physiol Rev* 2013;**93**:137–88
10. Lin Y, Berg AH, Iyengar P, Lam TKT, Giacca A, Combs TP, Rajala MW, Du X, Rollman B, Li W, Hawkins M, Barzilai N, Rhodes CJ, Fantus IG, Brownlee M, Scherer PE. The hyperglycemia-induced inflammatory response in adipocytes: the role of reactive oxygen species. *J Biol Chem* 2005;**280**:4617–26
11. Ghaisas S, Maher J, Kanthasamy A. Gut microbiome in health and disease: linking the microbiome-gut-brain axis and environmental factors in the pathogenesis of systemic and neurodegenerative diseases. *Pharmacol Ther* 2015;**158**:52–62
12. Cani PD, Osto M, Geurts L, Everard A. Involvement of gut microbiota in the development of low-grade inflammation and type 2 diabetes associated with obesity. *Gut Microbes* 2012;**3**:4:279–88
13. Amar J, Serino M, Lange C, Chabo C, Iacovoni J, Mondot S, Lepage P, Klopp C, Mariette J, Bouchez O, Perez L, Courtney M, Marre M, Klopp P, Lantieri O, Doré J, Charles M, Balkau B, Burcelin R. Involvement of tissue bacteria in the onset of diabetes in humans: evidence for a concept. *Diabetologia* 2011;**54**:3055–61
14. De Kort S, Keszthelyi D, Masclee AAM. Leaky gut and diabetes mellitus: what is the link? *Obes Rev* 2011;**12**:449–58
15. Prentki M, Nolan CJ. Islet beta cell failure in type 2 diabetes. *J Clin Invest* 2006;**116**:1802–12
16. Rhodes CJ. Type 2 diabetes - a matter of β-cell life and death? *Science* 2005;**307**:380–4
17. Sone H, Kagawa Y. Pancreatic beta cell senescence contributes to the pathogenesis of type 2 diabetes in high-fat diet-induced diabetic mice. *Diabetologia* 2005;**48**:58–67
18. Collares-Buzato CB. High-fat diets and β-cell dysfunction: molecular aspects. In: Mauricio D (eds) Molecular nutrition and diabetes. San Diego, USA: Elsevier, 2015, pp.115–130.
19. Oliveira RB, Maschio DA, Carvalho CPF, Collares-Buzato CB. Influence of gender and time diet exposure on endocrine pancreas remodeling in response to high fat diet-induced metabolic disturbances in mice. *Ann Anat* 2015;**200**:88–97
20. Oliveira RB, Carvalho CPF, Polo CC, Dorighello GG, Boschero AC, Oliveira HCF, Collares-Buzato CB. Impaired compensatory beta-cell function and growth in response to high-fat diet in LDL receptor knockout mice. *Int J Exp Pathol* 2014;**95**:296–308
21. Gómez-Dumm LA, Semino MC, Gagliardino JJ. Sequential morphological changes in pancreatic islets of spontaneously diabetic rats. *Pancreas* 1990;**5**:533–9
22. Cani PD, Bibiloni R, Knauf C, Neyrinck AM, Delzenne NM. Changes in gut microbiota control metabolic diet–induced obesity and diabetes in mice. *Diabetes* 2008;**57**:1470–81
23. Cani PD, Neyrinck AM, Fava F, Knauf C, Burcelin RG, Tuohy KM, Gibson GR, Delzenne NM. Selective increases of bifidobacteria in gut microflora improve high-fat-diet-induced diabetes in mice through a mechanism associated with endotoxaemia. *Diabetologia* 2007;**50**:2374–83
24. Al-Salami H, Butt G, Fawcett JP, Tucker IG, Golocorbin-Kon S, Mikov M. Probiotic treatment reduces blood glucose levels and increases systemic absorption of gliclazide in diabetic rats. *E*ur J Drug Metab Pharmacokinet 2008;**33**:101–6
25. Bosi E, Molteni L, Radaelli MG, Folini L, Fermo I, Bazzigaluppi E, Piemonti L, Pastore MR, Paroni R. Increased intestinal permeability precedes clinical onset of type 1 diabetes. *Diabetologia* 2006;**49**:2824–7
26. Neu J, Reverte CM, Mackey AD, Liboni K, Tuhacek-tenace LM, Hatch M, Li N, Caicedo RA, Schatz DA, Atkinson M. Changes in intestinal morphology and permeability in the BioBreeding rat before the onset of type 1 diabetes. *J Pediatr Gatroenterol Nutr* 2005;**40**:589–95
27. Meddings JB, Jarand J, Urbanski SJ, Hardin J, Gall DG. Increased gastrointestinal permeability is an early lesion in the spontaneously diabetic BB rat. *Am J Physiol* 1999;**276**:G951–7
28. Matsuzaki T, Nagata Y, Kado S, Uchida K, Kato I, Hashimoto S, Yokokura T. Prevention of onset in an insulin-dependent diabetes mellitus model, NOD mice, by oral feeding of Lactobacillus casei. *APMIS* 1997;**105**:643–9
29. Wang X, He G, Peng Y, Zhong W, Wang Y, Zhang B. Sodium butyrate alleviates adipocyte inflammation by inhibiting NLRP3 pathway. *Nat Sci Rep* 2015;**5**:1–10
30. Chang PV, Hao L, Offermanns S, Medzhitov R. The microbial metabolite butyrate regulates intestinal macrophage function via histone deacetylase inhibition. *Proc Natl Acad Sci* 2014;**111**:2247–52
31. Li HP, Chen X, Li MQ. Butyrate alleviates metabolic impairments and protects pancreatic beta cell function in pregnant mice with obesity. *Int J Clin Exp Pathol* 2013;**6**:1574–84
32. Hamer HM, Jonkers D, Venema K, Vanhoutvin S, Troost FJ, Brummer RJ. The role of butyrate on colonic function. *Aliment Pharmacol Ther* 2008;**27**:104–19
33. Inan MS, Rasoulpour RJ, Yin L, Hubbard AK, Rosenberg DW, Giardina C. The luminal short-chain fatty acid butyrate modulates NF-κB activity in a human colonic epithelial cell line. *Gastroenterology* 2000;**118**:724–34
34. Wang HB, Wang PY, Wang X, Wan YL, Liu YC. Butyrate enhances intestinal epithelial barrier function via up-regulation of tight junction protein claudin-1 transcription. *Dig Dis Sci* 2012;**57**:3126–35
35. Khan S, Jena G. Sodium butyrate reduces insulin-resistance, fat accumulation and dyslipidemia in type-2 diabetic rat: a comparative study with metformin. *Chem Biol Interact* 2016;**254**:124–34
36. Khan S, Jena GB. Protective role of sodium butyrate, a HDAC inhibitor on beta-cell proliferation, function and glucose homeostasis through modulation of p38/ERK MAPK and apoptotic pathways: study in juvenile diabetic rat. *Chem Biol Interact* 2014;**213**:1–12
37. Dudakovic A, Evans JM, Li Y, Middha S, McGee-Lawrence ME, Van Wijnen AJ, Westendorf JJ. Histone deacetylase inhibition promotes osteoblast maturation by altering the histone H4 epigenome and reduces Akt phosphorylation. *J Biol Chem* 2013;**288**:28783–91
38. Canani RB, Costanzo M Di, Leone L, Pedata M, Meli R, Calignano A. Potential beneficial effects of butyrate in intestinal and extraintestinal diseases. *World J Gastroenterol* 2011;**17**:1519–28
39. Gao Z, Yin J, Zhang J, Ward RE, Martin RJ, Lefevre M, Cefalu WT, Ye J. Butyrate improves insulin sensitivity and increases energy expenditure in mice. *Diabetes* 2009;**58**:1509–17
40. Falcão VTFL, Maschio DA, de Fontes CC, Oliveira RB, Santos-Silva JC, Almeida ACS, Vanzela EC, Cartaxo MT, Carvalho CPF, Collares-Buzato CB. Reduced insulin secretion function is associated with pancreatic islet redistribution of cell adhesion molecules (CAMs) in diabetic mice after prolonged high-fat diet. *Histochem Cell Biol* 2016;**146**:13–31
41. Carvalho CPF, Oliveira RB, Britan A, Santos-Silva JC, Boschero AC, Meda P, Collares-Buzato CB. Impaired β-cell-β-cell coupling mediated by Cx36 gap junctions in prediabetic mice. *Am J Physiol Endocrinol Metab* 2012;**303**:E144–51
42. Kim A, Miller K, Jo J, Kilimnik G, Wojcik P, Hara M. Islet architecture: a comparative study. *Islets* 2009;**1**:129–36
43. Catta-Preta M, Mendonca LS, Fraulob-Aquino J, Aguila MB, Mandarim-de-Lacerda CA. A critical analysis of three quantitative methods of assessment of hepatic steatosis in liver biopsies. *Virchows Arch* 2011;**459**:477–85
44. Castro AVB, Kolka CM, Kim SP, Bergman RN, Sinai C, Angeles L. Obesity, insulin resistance and comorbidities – mechanisms of association. *Arq Bras Endocrinol Metab* 2015;**58**:600–9
45. Cani PD, Amar J, Iglesias MA, Poggi M, Knauf C, Bastelica D, Neyrinck AM, Fava F, Tuohy KM, Chabo C, Waget A, Delmée E, Cousin B, Thierry Sulpice T, Chamontin B, Ferrières J, Tanti J-F, Gibson GR, Casteilla L, Delzenne NM, Alessi MC, Burcelin R. Metabolic endotoxemia initiates obesity and insulin resistance. *Diabetes* 2007;**56**:1761–72

46. Johnson AMF, Costanzo A, Gareau MG, Armando AM, Quehenberger O, Jameson JM, Olefsky JM. High fat diet causes depletion of intestinal eosinophils associated with intestinal permeability. *PLoS One* 2015;**10**:e0122195
47. Larsen N, Vogensen FK, Van Den Berg FWJ, Nielsen DS, Andreasen AS, Pedersen BK, Abu Al-Soud W, Sørensen SJ, Hansen LH, Mogens, Jakobsen M. Gut microbiota in human adults with type 2 diabetes differs from non-diabetic adults. *PLoS One* 2010;**5**:e9085
48. Suzuki T, Hara H. Dietary fat and bile juice, but not obesity, are responsible for the increase in small intestinal permeability induced through the suppression of tight junction protein expression in LETO and OLETF rats. *Nutr Metab* 2010;**7**:19
49. Henagan TM, Stefanska B, Fang Z, Navard AM, Ye J, Lenard NR, Devarshi PP. Sodium butyrate epigenetically modulates high-fat diet-induced skeletal muscle mitochondrial adaptation, obesity and insulin resistance through nucleosome positioning. *Br J Pharmacol* 2015;**172**:2782–98
50. Yki-Järvinen H. Nutritional modulation of non-alcoholic fatty liver disease and insulin resistance. *Nutrients* 2015;**7**:9127–38
51. Willebrords J, Veloso I, Pereira A, Maes M, Yanguas SC, Colle I, Van Den Bossche B, Da Silva TC, Oliveira CP, Andraus W, Alves VAF, Cogliati B, Vinken M. Strategies, models and biomarkers in experimental non-alcoholic fatty liver disease research. *Prog Lipid Res* 2015;**59**:106–25
52. Byrne CD, Olufadi R, Bruce KD, Cagampang FR, Ahmed MH. Metabolic disturbances in non-alcoholic fatty liver disease. *Clin Sci* 2009;**116**:539–64
53. Dankner R, Chetrit A, Shanik MH, Raz I, Roth J. Basal-state hyperinsulinemia in healthy normoglycemic adults is predictive of type 2 diabetes over a 24-year follow-up: a preliminary report. *Diabs Care* 2009;**32**:1464–6
54. Weyer C, Foley JE, Bogardus C, Tataranni PA, Pratley RE. Enlarged subcutaneous abdominal adipocyte size, but not obesity itself, predicts type II diabetes independent of insulin resistance. *Diabetologia* 2000;**43**:1498–506
55. Asghar Z, Yau D, Chan F, LeRoith D, Chan CB, Wheeler MB. Insulin resistance causes increased beta-cell mass but defective glucose-stimulated insulin secretion in a murine model of type 2 diabetes. *Diabetologia* 2006;**49**:90–9
56. Kato S, Ishida H, Tsuura Y, Tsuji K, Nishimura M, Horie M, Taminato T, Ikehara S, Odaka H, Ikeda I, Okada Y, Seino Y. Alterations in basal and glucose-stimulated voltage-dependent Ca^{2+} channel activities in pancreatic beta cells of non-insulin-dependent diabetes mellitus GK rats. *J Clin Invest* 1996;**97**:2417–25
57. Nagaraj V, Kazim A, Helgeson J, Lewold C, Barik S, Buda P, Reinbothe TM, Wennmalm S, Zhang E, Renström E. Elevated basal insulin secretion in type 2-diabetes caused by reduced plasma membrane cholesterol. *Mol Endocrinol* 2016;**30**:1059–69
58. Pinnick KE, Collins SC, Londos C, Gauguier D, Clark A, Fielding BA. Pancreatic ectopic fat is characterized by adipocyte infiltration and altered lipid composition. *Obesity* 2008;**16**:522–30
59. Valladares R, Sankar D, Li N, Williams E, Lai KK, Abdelgeliel AS, Gonzalez CF, Wasserfall CH, Larkin J III, Schatz D, Mark A, Atkinson AS, Triplett EW, Neu J, Lorca GL. Lactobacillus johnsonii N6.2 mitigates the development of type 1 diabetes in BB-DP rats. *PLoS One* 2010;**5**: e10507
60. Sapone A, De Magistris L, Pietzak M, Clemente MG, Tripathi A, Cucca F, Lampis R, Kryszak D, Cartenì M, Generoso M, Iafusco D, Prisco F, Laghi F, Riegler G, Carratu R, Counts D, Fasano A. Zonulin upregulation is associated with increased gut permeability in subjects with type 1 diabetes and their relatives. *Diabetes* 2006;**55**:1443–9
61. Fasano A. Zonulin and its regulation of intestinal barrier function: the biological door to inflammation, autoimmunity, and cancer. *Physiol Rev* 2011;**91**:151–75
62. Groschwitz KR, Hogan SP. Intestinal barrier function: molecular regulation and disease pathogenesis. *J Allergy Clin Immunol* 2009;**124**:3–20
63. Van Itallie CM, Anderson JM. Architecture of tight junctions and principles of molecular composition. *Semin Cell Dev Biol* 2014;**36**:157–65
64. Krug SM, Schulzke JD, Fromm M. Tight junction, selective permeability, and related diseases. *S*emin Cell Dev Biol 2014;**36**:166–76
65. Furuse M. Molecular basis of the core structure of tight junctions. *Cold Spring Harb Perspect Biol* 2010;**2**:a002907
66. Mukiza CN, Dubreuil DJ. Escherichia coli heat-stable toxin b impairs intestinal epithelial barrier function by altering tight junction proteins. *Infect Immun* 2013;**81**:2819–27
67. Cao M, Wang P, Sun C, He W, Wang F. Amelioration of IFN-γ and TNF-α-induced intestinal epithelial barrier dysfunction by berberine via suppression of MLCK-MLC phosphorylation signaling pathway. *PLoS One* 2013;**8**:e61944
68. Horton F, Wright J, Smith L, Hinton PJ, Robertson MD. Increased intestinal permeability to oral chromium (51Cr) -EDTA in human Type 2 diabetes. *Diab Med* 2014;**31**:559–63
69. Ding S, Chi MM, Scull BP, Rigby R, Schwerbrock NMJ, Magness S, Jobin C, Lund PK. High-fat diet: bacteria interactions promote intestinal inflammation which precedes and correlates with obesity and insulin resistance in mouse. *PLoS One* 2010;**5**: e12191
70. Huang C, Song P, Fan P, Hou C, Thacker P, Ma X. Dietary Sodium butyrate decreases postweaning diarrhea by modulating intestinal permeability and changing the bacterial communities in weaned piglets. *J Nutr* 2015;**21**:2274–80
71. Kumar M, Song H-J, Cho S-K, Balasubramanian S, Choe S-Y, Rho G-J. Effect of histone acetylation modification with sodium butyrate, a histone deacetylase inhibitor, on cell cycle, apoptosis, ploidy and gene expression in porcine fetal fibroblasts. *J Reprod Dev* 2007;**53**:903–13
72. Luo HM, Du MH, Lin ZL, Zhang L, Ma L, Wang H, Wen Yu W, Lv Y, Lu J-Y, Pi Y-L, Hu S, Sheng Z-Y. Valproic acid treatment inhibits hypoxia-inducible factor 1α accumulation and protects against burn-induced gut barrier dysfunction in a rodent model. *PLoS One* 2013;**8**:e77523
73. Vinken M, De Rop E, Decrock E, De Vuyst E, Leybaert L, Vanhaecke T, Rogiers V. Epigenetic regulation of gap junctional intercellular communication: more than a way to keep cells quiet? *Biochim Biophys Acta* 2009;**1795**:53–61

(Received February 4, 2017, Accepted April 10, 2017)